Multimode Laser Beam Field Correlations for Vertical Links Operating in Oceanic Turbulence

Gercekcioglu, Hamza; Baykal, Yahya; Gokce, Muhsin Caner

DOI
10.1109/JQE.2025.3568419

Publication date
2025

Document Version
Final published version

Published in
IEEE Journal of Quantum Electronics

Multimode Laser Beam Field Correlations for Vertical Links Operating in Oceanic Turbulence

Hamza Gerçekcioğlu, Yahya Baykal, and Muhsin Caner Gökçe

***Abstract*—In underwater optical vertical link medium, based on the extended Huygens-Fresnel principle, multimode laser beam field correlation is derived and evaluated analytically in the Atlantic Ocean at high latitude and high latitude- low latitudes. With the depth of seawater, the coherence length of a spherical wave operating in the underwater turbulent medium is demonstrated for the range of 0-4000 m. By utilizing the coherence length varying with parameters such as the rate of dissipation of turbulent kinetic energy per unit mass of fluid ε, the rate of dissipation of the mean squared temperature χ_T and non-dimensional representing the relative strength of temperature and salinity fluctuations ω, which depend on depth, the field correlation is examined in detail for single modes and multimode. Their variations are exhibited. Our results indicate clearly that as the mode increases, field correlation gets better.**

***Index Terms*—Oceanic turbulence, coherence length, intensity, oceanic vertical link, multimode beam.**

I. Introduction

THERE are important searches and studies on optical communication links for the factors such as bandwidth, for preventing the distortion of waves transmitted through communication media, and information security. Hence, the propagation of laser beams both in a turbulent atmosphere and in a turbulent underwater environment has attracted substantial attention due to their wide applications in free space optical communication links, in oceanic optical communication links and remote sensing. Moreover, many studies are reported on the propagation of various coherent and partially coherent laser beams in a turbulent atmosphere [1], [2], [3], [4], [5], [6], [7], [8], [9], [10], [11], [12], [13], [14], [15], [16], [17], [18] and in a turbulent underwater medium [19], [20]. In this context, naturally many studies have been conducted on multimode [12], [13], [14], [16], [20]. With the studies on multimode, the importance of this beam type is revealed [14], [21], [22], [23], [24], [25]. With this study being one of the first studies on multimode and mentioned in [14], scintillation index is derived and calculated and the advantages of multimode are carried out. Scintillation index of multimode and of the Hermite Gaussian beam mode field profile are investigated for air vehicle communication systems in vertical links of weak atmospheric turbulent conditions [24], [25]. We have studied the bit error rate of focused Gaussian beam and of collimated annular beam in horizontal links and M-pulse position modulated Gaussian beam in vertical links operating in weak oceanic turbulent medium [26], [27], [28].

Inspired by the above-mentioned studies and [28], [29], and [30], it is desired to investigate the multimode field correlations in the vertical links in the Atlantic and the Pacific oceanic turbulent environments. As far as we know, multimode field correlations in the vertical links have not been reported. In this study, the influences of this beam parameters and oceanic turbulence on the average intensity of multimode field have been examined by using the numerical examples in detail. This study based on factual information is reported for the first time and obtained results can inspire many important optical applications.

Received 22 November 2024; revised 7 March 2025 and 15 April 2025; accepted 25 April 2025. Date of publication 9 May 2025; date of current version 20 June 2025. *(Corresponding author: Hamza Gerçekcioğlu.)*

Hamza Gerçekcioğlu is with the Ministry of Transport and Infrastructure, 06100 Ankara, Türkiye (e-mail: hgercekcioglu@hotmail.com).

Yahya Baykal is with the Electrical-Electronics Engineering Department, Çankaya University, 06790 Ankara, Türkiye (e-mail: y.baykal@cankaya.edu.tr).

Muhsin Caner Gökçe is with the Electrical-Electronics Engineering Department, TED University, 06420 Ankara, Türkiye, and also with the Department of Geoscience and Remote Sensing, Delft University of Technology, 2628 CD Delft, The Netherlands (e-mail: muhsin.Gökce@tedu.edu.tr).

Digital Object Identifier 10.1109/JQE.2025.3568419

II. Formulation

A. Incident Optical Field

The multimode laser beam incident field, i.e., $u^{inc}(s)$, is stated by [23]

$$u^{inc}\left(s_x, s_y\right) = \sum_{(n,m)} u^{inc}_{nm}\left(s_x, s_y\right), \tag{1}$$

where $\sum_{(n,m)}$ is the summation of the single mode incident fields with index nm and

$$u^{inc}_{nm}\left(s_x, s_y\right) = H_n\left(s_x/\alpha_s\right) H_m\left(s_y/\alpha_s\right) \exp\left[-\left(s_x^2 + s_y^2\right)/2\alpha_s^2\right], \tag{2}$$

indicates the single mode field. Here H_n and H_m are the Hermite polynomials of order n and m providing the field distributions in the s_x, s_y directions, α_s being the source size, nm symbolizes the mode indices. Field correlations of the multimode laser beam incidence in oceanic turbulent is given by $< u_s\left(p_{x_1}, p_{y_1}, L\right) u_s^*\left(p_{x_2}, p_{y_2}, L\right) >$ where $u_s\left(p_x, p_y, L\right)$ is the field at the transverse receiver plane, <.> and * denoting the ensemble average and the complex conjugate, respectively.

B. Receiver Optical Field

Using the extended Huygens-Fresnel principle, the field at the receiver plane is found as [1],

$$\begin{aligned} & u\left(p_x, p_y, L\right) \\ & = \frac{\exp(ikL)}{\lambda i L} \int_{-\infty}^{\infty} \int_{-\infty}^{\infty} \mathrm{d}s_x \mathrm{d}s_y u\left(s_x, s_y\right) \\ & \quad \times \exp\left(ik\left[\left|s_x - p_x\right|^2 + \left|s_y - p_y\right|^2\right]/2L\right) \\ & \quad \exp\left[\psi\left(s_x, p_x\right) + \psi\left(s_y, p_y\right)\right], \end{aligned} \tag{3}$$

Here $i = \sqrt{-1}, L$ is the propagation length, $k = 2\pi/\lambda$ is the propagation constant, λ being the wavelength. $\psi(s_x, p_x)$ and $\psi\left(s_y, p_y\right)$ are the random complex phase of a spherical wave transmitting x and y directions between the source point and the receiver point in the turbulent oceanic medium. Field correlations of the multimode laser beam incidence in oceanic turbulent is expressed by

$$\begin{aligned} & < u\left(p_{x_1}, p_{x_1}, L\right) u^*\left(p_{x_2}, p_{y_2}, L\right) > \\ & = \frac{1}{(\lambda L)^2} \int_{-\infty}^{\infty} \int_{-\infty}^{\infty} \int_{-\infty}^{\infty} \int_{-\infty}^{\infty} ds_{x_1} ds_{y_1} ds_{x_2} ds_{y_2} \\ & \quad u\left(s_{x_1}, s_{y_1}\right) u^*\left(s_{x_2}, s_{y_2}\right) \\ & \quad \times \exp\left(ik\left|s_{x_1} - p_{x_1}\right|^2/2L\right) \exp\left(ik\left|s_{y_1} - p_{y_1}\right|^2/2L\right) \\ & \quad \times \exp\left(ik\left|s_{x_2} - p_{x_2}\right|^2/2L\right) \exp\left(ik\left|s_{y_2} - p_{y_2}\right|^2/2L\right) \\ & \quad \times < \exp\left[\psi\left(s_{x_1}, p_{y_1}\right) + \psi\left(s_{y_1}, p_{y_1}\right)\right] \\ & \quad \exp\left[\psi^*\left(s_{x_2}, p_{x_2}\right) + \psi^*\left(s_{y_2}, p_{y_2}\right)\right] > \end{aligned} \tag{4}$$

where

$$\begin{aligned} & < \exp\left[\psi\left(s_{x_1}, p_{x_1}\right) + \psi\left(s_{y_1}, p_{\gamma_1}\right)\right] \\ & \quad \exp\left[\psi^*\left(s_{x_1}, p_{x_2}\right) + \psi^*\left(s_{y_2}, p_{y_2}\right)\right] > \\ & = \exp\left[-\left(\left|s_{x_1} - s_{x_2}\right|^2 + \left|s_{\gamma_1} - s_{\gamma_2}\right|\right.\right. \\ & \quad \left.\left. \cdot \left|p_{x_1} - p_{x_2}\right| + \left|p_{\gamma_1} - p_{\gamma_2}\right|^2\right)/\rho_0^2(h)\right] e \end{aligned} \tag{5}$$

Here $\rho_0(h)$ is the coherence length of a spherical wave propagating in the underwater turbulent medium and h is the depth of seawater, that is, $h = 0$ is the sea surface. Coherence length of a spherical wave propagating in the turbulent medium is defined as [31],

$$\rho_0(h) = \left[\frac{\pi^2 k^2 L}{3} \int_0^{\infty} \kappa^3 \Phi(h, \kappa) \mathbf{d}\kappa\right]^{-1/2} \tag{6}$$

where $\kappa \exp(i\psi)$ is the two dimensional spatial frequency in polar coordinates, κ is the magnitude. The spatial power spectrum of turbulent fluctuations of the seawater refraction index of vertical underwater links, $\Phi_n(h, \kappa)$, is derived, which is expressed as Eq. (1) in [29]. Inserting Eq. (1) stated in [4] into Eq. (6) and performing the integration, coherence length is found as [31]

$$\begin{aligned} \rho_0(h) = |\omega(h)| & \left\{1.802 \times 10^{-7} k^2 L\left[\varepsilon(h)\eta_s(h)\right]^{-1/3}\right. \\ & \left.\times \chi_{\mathrm{T}}(h)\left[0.483\omega^2(h) - 0.835\omega(h) + 3.38\right]\right\}^{-0.5} \end{aligned} \tag{7}$$

where $\omega(.)$ is unit less, relative strength of temperature and salinity fluctuations parameter, representing the ratio of temperature to salinity contributions to the refractive index spectrum, $\chi_T(.)$ is the rate of dissipation of mean-squared temperature in K^2/s, $\varepsilon(.)$ is the rate of dissipation of kinetic energy per unit mass of fluid in m^2/s^3 and $\eta_s(.)$ is the inner scale, i.e., Kolmogorov microscale, which obtained in

$$\begin{aligned} I_{12x}(p, L) = \pi \exp & \left(\frac{f_{12x}^2}{4\beta_{1x}}\right) \sum_{t_{n1}=0}^{n_1/2} \sum_{t=0}^{(n_1-2t_{n1})/2} \sum_{t_1=0}^{(n_1-2t_{n1}-2t)} \sum_{t_{n2}=0}^{n_2/2} (-1)^t i^{-n_1-n_2+t_1} \\ & \times \frac{n_1! n_2!}{t! t_1! t_{n1}! t_{n2}! (n_1 - 2t_{n1} - 2t - t_1)! (n_2 - 2t_{n2})!} \alpha_s^{-(n_1-n_2-2t_{n1}-2t_{n2})} \\ & \times \beta_{1x}^{-(n_1-n_2+t_1-2t_{n1}+2t_{n2})/2} f_{12x}^{t_1} \rho_0^{2(1+n_2-2t_{n2})} \left(\beta_{1x}^* \rho_0^4 \beta_{1x} - 1\right)^{-(1+n_1-2t_{n1}-2t-t_1+n_2-2t_{n2})/2} \\ & \times \exp\left[\frac{\left(\gamma_x \rho_0^2 \beta_{1x} + 1\right)^2}{4\beta_{1x}\left(\beta_{1x}^* \rho_0^4 \beta_{1x} - 1\right)}\right] \mathrm{H}_{(n_1-2t_{n1}-2t-t_1+n_2-2t_{n2})}\left[\frac{i\left(\gamma_x \rho_0^2 \beta_{1x} + 1\right)}{\sqrt{4\beta_{1x}\left(\beta_{1x}^* \rho_0^4 \beta_{1x} - 1\right)}}\right] \end{aligned} \tag{9}$$

$$\begin{aligned} I_{12y}(p, L) = \pi \exp & \left(\frac{f_{12y}^2}{4\beta_{1y}}\right) \sum_{t_{m1}=0}^{m_1/2} \sum_{t=0}^{(m_1-2t_{m1})/2} \sum_{t_1=0}^{(m_1-2t_{m1}-2t)} \sum_{t_{m2}=0}^{m_2/2} (-1)^t i^{-m_1-m_2+t_1} \\ & \times \frac{m_2! m_1!}{t! t_1! t_{m2}! t_{m1}! (m_1 - 2t_{m1} - 2t - t_1)! (m_2 - 2t_{m2})!} \alpha_s^{-(m_1+m_2-2t_{m1}-2t_{m2})} \\ & \times \beta_{1y}^{-(m_1-m_2+t_1-2t_{m1}+2t_{m2})/2} f_{12y}^{t_1} \rho_0^{2(1+m_2-2t_{m2})} \left(\beta_{1y}^* \rho_0^4 \beta_{1y} - 1\right)^{-(1+m_1-2t_{m1}-2t-t_1+m_2-2t_{m2})/2} \\ & \times \exp\left[\frac{\left(\gamma_y \rho_0^2 \beta_{1y} + 1\right)^2}{4\beta_{1y}\left(\beta_{1y}^* \rho_0^4 \beta_{1y} - 1\right)}\right] \mathrm{H}_{(m_1-2t_{m1}-2t-t_1+m_2-2t_{m2})}\left[\frac{i\left(\gamma_y \rho_0^2 \beta_{1y} + 1\right)}{\sqrt{4\beta_{1y}\left(\beta_{1y}^* \rho_0^4 \beta_{1y} - 1\right)}}\right] \end{aligned} \tag{10}$$

TABLE I
THE PARAMETERS OF THE SIMULATIONS

$\lambda = 532\ nm,\ \eta_s = 5\text{x}10^{-3}$ m, $p_{1x} = p_{1y} = 10^{-3}$ m, $\alpha_s = 5$ cm	
Figure 1	$0-4000\ m,\ \varsigma^0 = 0^0$
Figure 2	$0-4000\ m, \varsigma^0 = 0,\ 30^0,\ 60^0$
Figures 3-8	$3300\ m-3500\ m, \varsigma^0 = 0^0$
Figure 9	$3700\ m-3500\ m, \varsigma^0 = 0^0$
Figure 10	$3700\ m-3500\ m, \varsigma^0 = 0^0$
Figure 11	$3700\ m-3500\ m, \varsigma^0 = 0^0$
Figures 12-14	$3300\ m-3500\ m, -60^0 \le \varsigma^0 \le 60^0$
Figure 15	$3500\ m-3700\ m, \varsigma^0 = 0^0$

[32] by the use of the Nikishov-Nikishov power spectrum of underwater turbulence [33].

$$
\begin{aligned}
&< u(p_1, L)\, u*(p_2, L) \\
&>= \frac{1}{(\lambda L)^2} \exp\left\{\frac{ik}{2L}\left[\left(p_{1x}^2 + p_{1y}^2\right) - \left(p_{2x}^2 + p_{2y}^2\right)\right]\right. \\
&\quad \left. - \frac{1}{\rho_0^2}\left[(p_{1x} - p_{2x})^2 + \left(p_{1y} - p_{2y}\right)^2\right]\right\} \\
&\quad \times \sum_{(n_1,m_1)}^{N_s} \sum_{(n_2,m_2)}^{N_s} A_{n_1 m_1} A^*_{n_2 m_2} I_{12x}(p, L)\, I_{12y}(p, L), \qquad (8)
\end{aligned}
$$

where, (9) and (10), as shown at the bottom of the previous page, and

$$\beta_{1x} = \beta_{1y} = -\frac{ik}{2L} + \frac{1}{2\alpha_s^2} + \frac{1}{\rho_0^2}, \qquad (11a)$$

$$
\begin{aligned}
f_{12x} &= -\frac{ikp_{1x}}{L} - \frac{1}{\rho_0^2}(p_{1x} - p_{2x}), f_{12y} \\
&= -\frac{ikp_{1y}}{L} - \frac{1}{\rho_0^2}\left(p_{1y} - p_{2y}\right), \qquad (11b)
\end{aligned}
$$

$$
\begin{aligned}
\gamma_x &= \frac{ik}{L}p_{2x} + \frac{1}{\rho_0^2}(p_{1x} - p_{2x}), \gamma_y \\
&= \frac{ik}{L}p_{2y} + \frac{1}{\rho_0^2}\left(p_{1y} - p_{2y}\right), \qquad (11c)
\end{aligned}
$$

Considering the propagation length L, it is noted that the depth of the seawater will be defined as $h = h_0 + L\cos\left(\varsigma^0\right)$ for the slant downlink, and as $h = h_0 - L\cos\left(\varsigma^0\right)$ for slant uplink, where $h = h_0$ is the initial depth level point and ς^0 is the zenith angle. By inserting the corresponding h in $\Phi_n(h, \kappa)$, we obtain depth dependent spatial power spectrum of turbulent fluctuations of the seawater refraction index, i.e., $\Phi_n(h, \kappa)$ which is used in Eq. (6). It can be shown that our formulation can be correctly reduced to vertical and horizontal links when $\varsigma^0 = 0^0$ and $\varsigma^0 = 90^0$, respectively.

III. NUMERICAL RESULTS

The formulation of multimode laser beam field correlations is derived analytically for vertical links operating in oceanic turbulence. By using $r = \left(r_x, r_y\right)$, $p_{2x} = p_{1x} + r$ is taken, i.e., $\left(p_{2x}, p_{2y}\right) = \left(p_{1x} + r_x, p_{1y} + r_y\right)$. The average receiver intensity at selected propagation length are normalized by the same quantity as

$$
\begin{aligned}
&< u\left(p_{x_1}, p_{y_1}\right) u*\left(p_{x_2}, p_{y_2}\right) > \\
&=< u_s\left(p_{x_1}, p_{y_1}\right) u_s^*\left(p_{x_2}, p_{y_2}\right) > / \\
&\max\left[< u_s\left(p_{x_1}, p_{y_1}\right) u_s^*\left(p_{x_2}, p_{y_2}\right)\right] \qquad (12)
\end{aligned}
$$

In Table I, the parameters used in the simulations reflected in the figures of this section are provided. Other necessary information employed in the figures is provided in the legend, axes titles and captions of each figure.

Eq. (12) represents the average field correlations of multimode fields due to oceanic turbulence only. However, in the ocean, in addition to turbulence scattering, there are also substantial attenuation arising from scattering and absorption from oceanic particles. Thus, average field correlations are also exposed to additional attenuations due to particle scattering and particle absorption which are given by factors of $e^{-\sigma_{sc}(\lambda)L}$ and $e^{-\sigma_{abs}(\lambda)L}$, respectively. Here $\sigma_{sc}(\lambda)$ and $\sigma_{abs}(\lambda)$ are the scattering and absorption coefficients of oceanic particles,

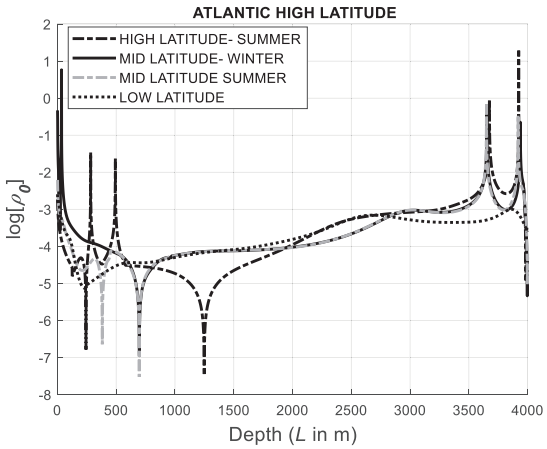

Fig. 1. The coherence length depth of a spherical wave propagating in the underwater turbulent medium for the Atlantic Ocean at high, mid and low latitudes.

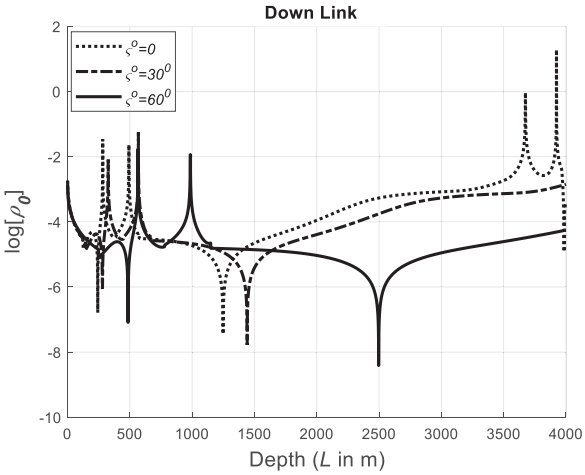

Fig. 2. The coherence length depth of a spherical wave propagating for various zenith angle ς^0 in downlink in the Atlantic Ocean high latitude-low latitudes.

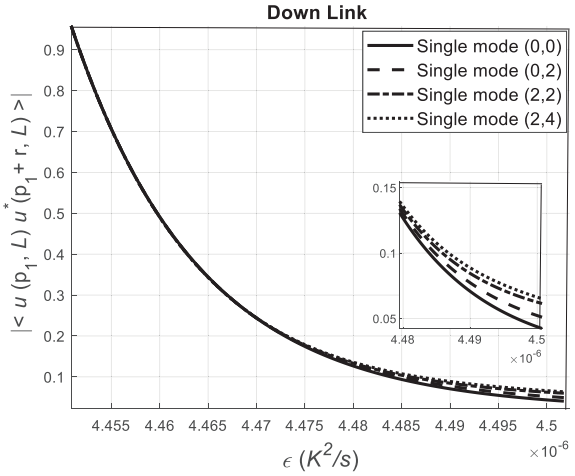

Fig. 3. Field correlations against various rate of dissipation of turbulent kinetic energy per unit mass of fluid ε for different even order single modes.

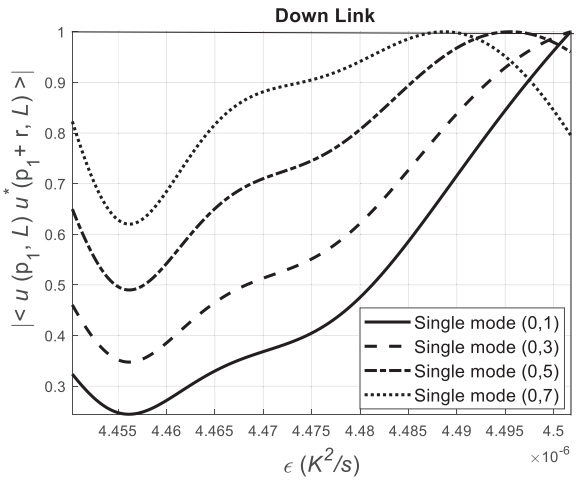

Fig. 4. Field correlations against various rate of dissipation of turbulent kinetic energy per unit mass of fluid ε for different odd order single modes.

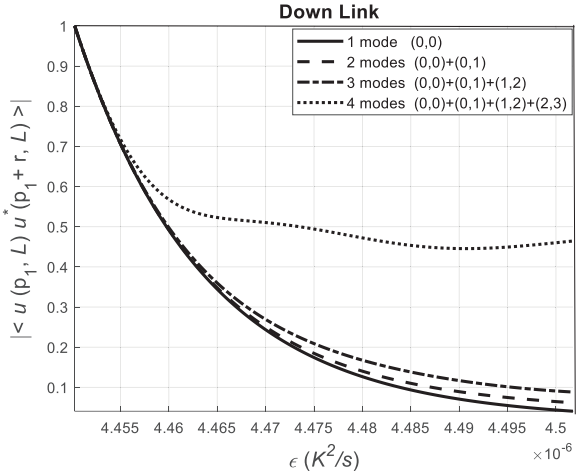

Fig. 5. Field correlations against various rate of dissipation of turbulent kinetic energy per unit mass of fluid ε for different multimode orders.

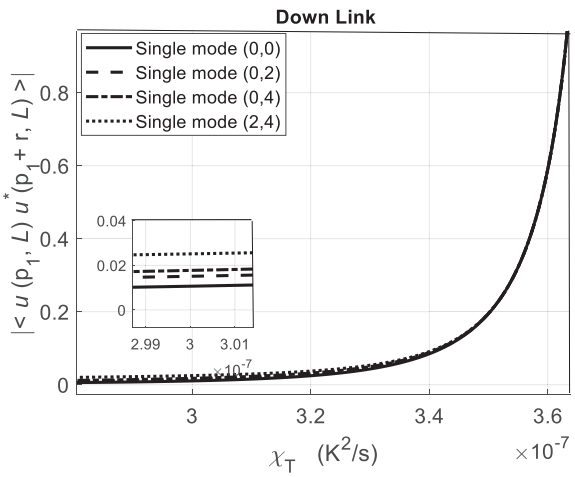

Fig. 6. Field correlations against the rate of dissipation of the mean squared temperature χ_T for down link at selected different single modes.

respectively which depend on the type of water and are functions of wavelength. The main purpose in this paper is to understand the behavior of the average field correlations of multimode fields for vertical links in oceanic turbulence so the figures in this section present turbulence effects. However, for completeness, in Fig. 15, in addition to oceanic turbulence effects, in the field correlations, we also incorporate the scattering and absorption effects arising from the oceanic particles as well.

Considering Eq. (12), the results are obtained through Eq. (11) by inserting Eqs. (2) and (9) and shown at the selected values including source size, i.e., α_s = 5cm. It is considered that specific medium is the Atlantic Ocean at high latitude and high latitude- low latitudes, which is widely examined in detail in [29] and [30]. While the figures related to $\varepsilon(.)$, $\chi_T(.)$ and zenith angle are drawn for the propagation distance range between depth of 3300 m and depth of 3500 m, in order for the figures related to ω to be clearly visible, the propagation distance range is taken between 3500 m and 3700 m depth. Based on Eq. (7), Fig. 1 and Fig. 2 are shown for the behavior of the coherence length of a spherical wave, i.e., ρ_0, propagating in the selected media at the vertical range of 0 - 4000 m, with various zenith angle selected as $\varsigma^0 = 0, 30^0, 60^0$ in the oceanic high latitude-low latitudes medium. It is observed that as the zenith angle increases, the features and changes at the coherence radius are also shifted. Fig. 3, Fig. 4 and Fig. 5 are depicted for field correlations versus various rate of dissipation of turbulent kinetic energy per unit mass of fluid ε for even and odd order single modes and multimode at underwater down link medium, respectively. In Fig. 3 and Fig. 4, it is observed that the improvement increases with the increase in the mode order number. That is, the increase in the number of mode orders contributes significantly to the reduction of the turbulence effect of the environment. In Fig. 5, the advantage of multimode, which has the highest order, i.e., (0,0) +(0,1) +(1,2) +(2,3), over others is clearly seen. The increase in rate of dissipation of turbulent kinetic energy per unit mass of fluid ε leads to affect the beam propagation, i.e.,. the laser beam field correlations. Including Fig. 5, for each value taken, the field correlations

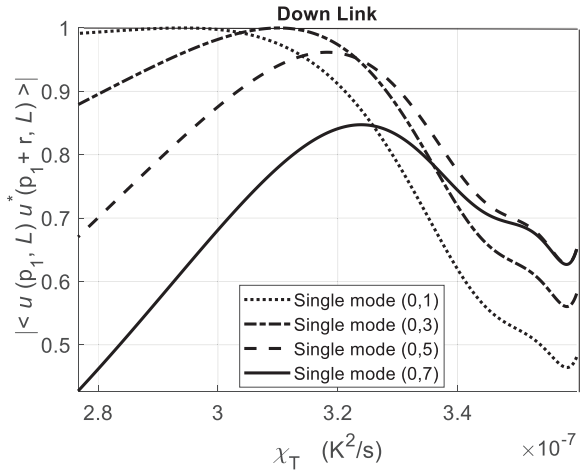

Fig. 7. Field correlations against the rate of dissipation of the mean squared temperature χ_T for uplink at selected different single modes.

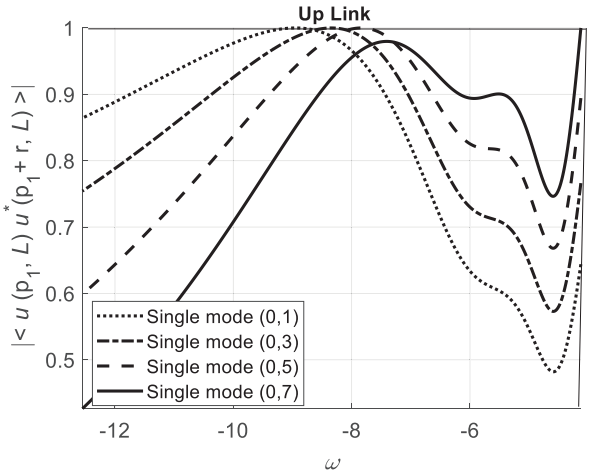

Fig. 9. Field correlations against non-dimensional representing the relative strength of temperature and salinity fluctuations ω for down link at selected different odd order single modes.

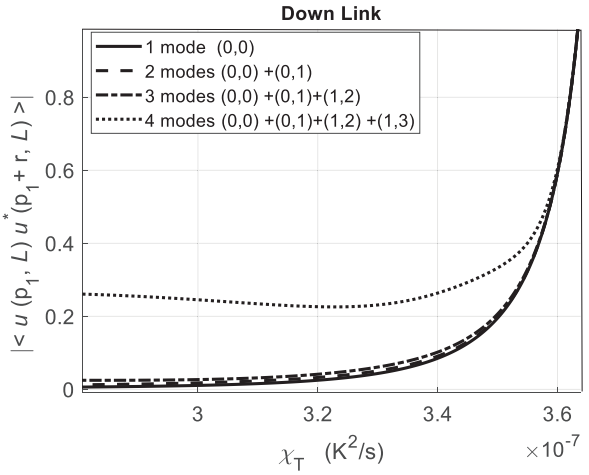

Fig. 8. Field correlations against the rate of dissipation of the mean squared temperature χ_T for down link at selected different multimode orders.

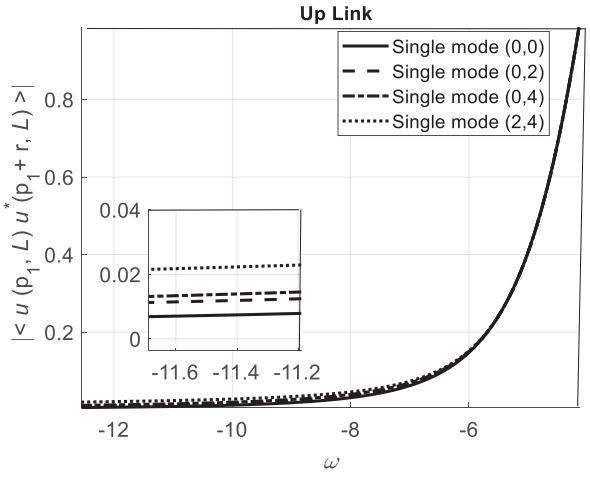

Fig. 10. Field correlations against non-dimensional representing the relative strength of temperature and salinity fluctuations ω for down link at selected different even order single modes.

should be considered and interpreted as a separate range, and even the fact that odd orders and even orders do not show similar properties should be attributed to this. Naturally, this feature is also observed in other figures, i.e., in Figs 6–14.

For the down link, field correlations versus the rate of dissipation of the mean squared temperature χ_T at the selected different single modes involved in even and odd modes are drawn in Fig. 6 and 7. The field correlation including even and odd modes exhibits different characteristic features. While the rate of dissipation of the mean squared temperature χ_T at selected different single modes involved in even order increases, an increment at the field correlations is observed drastically. Controversially, at the chosen different single odd modes, the increase in the rate of dissipation of the mean squared temperature slightly reduces the field correlations at before approximately $\chi_T = 3.2\text{x}10^{-7}$.However, after that value, it remarkable rises with the growth of orders in Fig. 7. As shown in Fig. 8, the multimode beams having even and odd number of modes causes field correlations at the receiver plane lead to results that exhibit growing trends. Single even modes appear to be dominant. The advantage of multimode possessing the highest order, i.e., (0,0) +(0,1) +(1,2) +(2,3) is obviously observed over others. Figs. 9, 10 and 11 are depicted for field correlations against non-dimensional representing the relative strength of temperature and salinity fluctuations ω for uplink at selected different odd order single modes, even order single modes and multimode orders, respectively. Especially, the propagation distance ranges are selected between depth of 3700 m and depth of 3500 m in order to clearly see the characteristics of attitude of the relative strength of temperature and salinity fluctuations. In Fig. 9, being up to $\omega = -8$, the increase in order causes a decrease in the field correlation. After $\omega = -8$, there is a gradual increase in the field correlation. Whereas, in Fig. 10, the increase in order causes a arise in the field correlation. The increase in ω value provides best results for the field correlation by examining multimode defined as (0,0)+(0,1) +(1,2) +(2,3), as well as seen Fig. 11. Fig. 12, 13 and 14 are drawn for the field

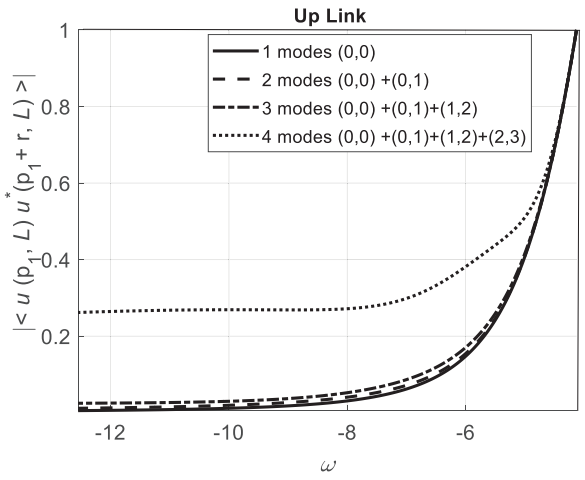

Fig. 11. Field correlations against non-dimensional representing the relative strength of temperature and salinity fluctuations ω for down link at selected multimode orders.

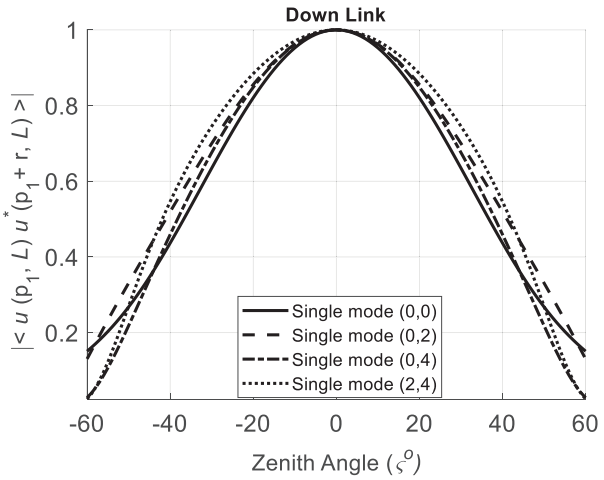

Fig. 12. Field correlations against zenith angle for down link at selected different even order single modes.

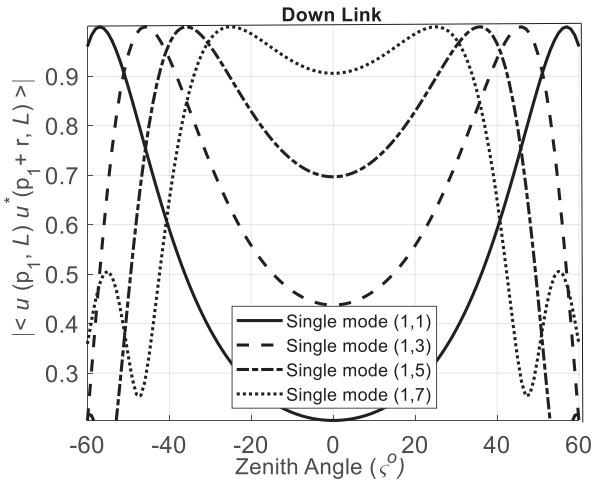

Fig. 13. Field correlations against zenith angle for down link at selected different odd order single modes.

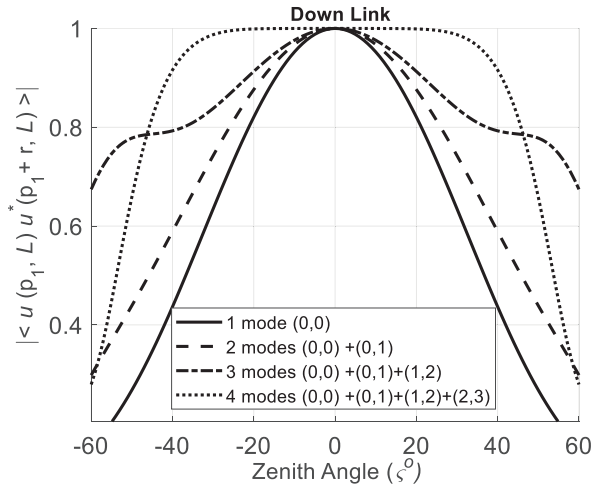

Fig. 14. Field correlations against zenith angle for down link at selected different multimode orders.

correlations against zenith angle for down link at selected different even and odd order single modes and multimode, respectively. It is noted that when $\omega(.)$ being the relative strength of temperature and salinity fluctuations parameter goes to infinitive, Nikishov-Nikishov power spectrum reduces to the spectrum of the temperature fluctuation. When $\omega(.)$ also approaches to zero, the power spectrum degrades into the spectrum of the salinity fluctuation, Moreover, the minus sign of the quantity $\omega(.)$ indicates that is a reduction in temperature and an increase in salinity with depth [29], [30], [34], [35]. For Fig. 12, it is difficult to say anything about field correlation by looking at the change in single mode. However, it is seen that field correlation decreases with increasing zenith angle. The increase in single mode clearly results in an improvement of field correlation. That is, it is observed that while zenith angle goes from zero to $\varsigma^0 = \pm 60^0$, field correlations increase by accelerating odd order. In Fig. 14, the increase in the modes causes the field correlations to arise in chosen the angle range. While modes pass from single mode to four multimode, the field correlation is improved by widening the zenith angle from $\varsigma^0 = 0^0$ to about $\varsigma^0 = 40^0$ with (0,0)+(0,1) +(1,2) +(2,3) modes. The results obtained through Eqs. (7) and (2) are shown for vertical paths at the selected odd and even orders that can be compared with each other for single mode. While Figs. (3)–(8) are demonstrated for the rate of dissipation of turbulent kinetic energy per unit mass of fluid ε and the rate of dissipation of the mean squared temperature χ_T for down link, Figs. (9)–(11) are depicted for unitless, relative strength of temperature and salinity fluctuations parameter ω for uplink. In fact they reflect variations for vertical propagation length, i.e., depth, since ε, χ_T and ω depend on depth, i.e., ε, χ_T and ω are functions of depth [29], [30].

Fig. 15 is drawn to introduce also the attenuation effect due to scattering and absorption originating from particles in the ocean to the field correlations for the down link. The scattering and absorption coefficients of oceanic particles, $\sigma_{sc}(\lambda)$ and $\sigma_{abs}(\lambda)$ are chosen to be 0.00218 and 0.05172, which are the interpolated values for the oceanic pure saltwater at the wavelength of 532 nm obtained from the data given

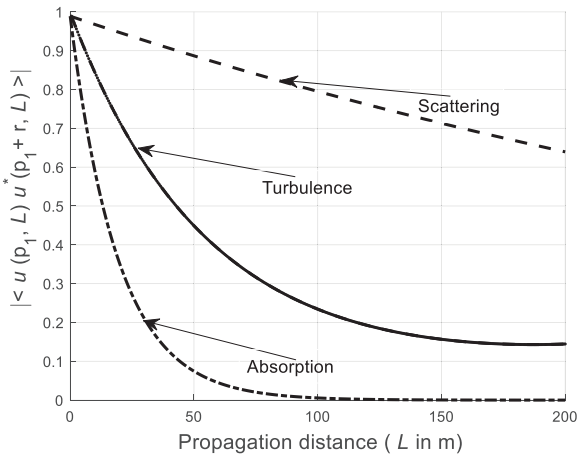

Fig. 15. Turbulence, particle scattering and absorption effects on the field correlations of the laser beam against propagation length for down link.

in [36]. Since there is no exact data at the wavelength of 532 nm, interpolation is applied that naturally brings some inaccuracy in the coefficients. However, this inaccuracy is almost negligible. In Fig. 15, it is seen that the absorption attenuation is much larger than the scattering attenuation at this range of propagation distances, that is, when the range of depth is from 3500 m to 3700 m.

IV. Conclusion

This study aims to demonstrate the behavior of multimode laser beam field correlations for vertical links in underwater turbulent medium mentioned as the Atlantic Ocean at high latitude and high latitude- low latitudes. In addition to exhibiting the behavior of the multimode beam, the coherence length of a spherical wave propagating in this environment is also shown for the vertical link. Based on the extended Huygens-Fresnel principle, multimode laser beam field correlations are investigated, and its formulation is derived analytically and evaluated. All figures, except for those related to coherence length, are obtained by appraising this formulation. Considering the feature of the underwater parameter possessing an important place in the field correlation and coherence length equation, mentioned in [29] and [30], laser beam propagation distance range, except for Figs. (9)–(11), is selected from depth of 3300 m and depth of 3500 m for the down link, or from depth of 3700 m and depth of 3500 m for the uplink. When the coherence characteristic is examined, characteristic shifts are observed with the increase in the zenith angle. In addition, when the field correlations versus various rate of dissipation of turbulent kinetic energy per unit mass of fluid ε, the rate of dissipation of the mean squared temperatureχ_T and unit less, relative strength of temperature and salinity fluctuations parameter ω, which indirectly express each depth, laser beams with mode have more advantage than Gaussian laser beams having (0,0). The increase in the number of modes results in an improvement in the field correlation. In addition, the multimode obtains remark advantageous field correlations. The results, presented in this study being on the improvement of the field correlation, are as clear as desired, except for Fig. 12.This information will be useful for optical system design including various optical applications which comprise LIDAR, microscopy, interferometry, imaging, optical and quantum communications, especially in underwater turbulent medium.

In this study, we did not perform experiments. Also, to our knowledge, there are no reported experiments in the literature in this field of multimode laser beam field correlations for vertical links operating in oceanic turbulence to validate our presented results. However, our work in this paper will provide important information which will form a significant basis for future experimental studies.

References

[1] L. C. Andrews and R. L. Philips, *Laser Beam Propagation Through Random Media, Second Edition*, 2nd ed., Bellingham, WA, USA: SPIE, 2005.

[2] S. C. H. Wang and M. A. Plonus, "Optical beam propagation for a partially coherent source in the turbulent atmosphere," *J. Opt. Soc. Amer.*, vol. 69, no. 9, p. 1297, 1979, doi: 10.1364/josa.69.001297.

[3] Y. Baykal and M. A. Plonus, "Intensity fluctuations due to a spatially partially coherent source in atmospheric turbulence as predicted by Rytov's method," *J. Opt. Soc. Amer. A, Opt. Image Sci.*, vol. 2, no. 12, p. 2124, 1985, doi: 10.1364/josaa.2.002124.

[4] Y. Baykal, "Formulation of correlations for general-type beams in atmospheric turbulence," *J. Opt. Soc. Amer. A, Opt. Image Sci.*, vol. 23, no. 4, p. 889, 2006, doi: 10.1364/josaa.23.000889.

[5] Y. Mizuno, K. Ohi, T. Sogabe, Y. Yamamoto, and Y. Kaneda, "Four-point correlation function of a passive scalar field in rapidly fluctuating turbulence: Numerical analysis of an exact closure equation," *Phys. Rev. E, Stat. Phys. Plasmas Fluids Relat. Interdiscip. Top.*, vol. 82, no. 3, Sep. 2010, Art. no. 036316, doi: 10.1103/physreve.82.036316.

[6] Y. Baykal, "Sinusoidal Gaussian beam field correlations," *J. Opt.*, vol. 14, no. 7, Jul. 2012, Art. no. 075707, doi: 10.1088/2040-8978/14/7/075707.

[7] Y. Baykal, Y. Cai, and X. Ji, "Field correlations of annular beams in extremely strong turbulence," *Opt. Commun.*, vol. 285, nos. 21–22, pp. 4171–4174, Oct. 2012, doi: 10.1016/j.optcom.2012.07.006.

[8] M. Nairat and D. Voelz, "Propagation of rotational field correlation through atmospheric turbulence," *Opt. Lett.*, vol. 39, no. 7, p. 1838, 2014, doi: 10.1364/ol.39.001838.

[9] Y. Baykal, "Field correlations of laser arrays in atmospheric turbulence," *Appl. Opt.*, vol. 53, no. 7, p. 1284, Mar. 2014, doi: 10.1364/ao.53.001284.

[10] Z. Liu and D. Zhao, "Propagation of partially coherent vortex beams in atmospheric turbulence by a spatial light modulator," *Laser Phys. Lett.*, vol. 16, no. 5, Apr. 2019, Art. no. 056003, doi: 10.1088/1612-202x/ab0a6b.

[11] T. Wang, "Propagation of partially coherent vortex beams in a turbulent atmosphere," *Opt. Eng.*, vol. 47, no. 3, Mar. 2008, Art. no. 036002, doi: 10.1117/1.2896309.

[12] Y. Yuan, Y. Cai, J. Qu, H. T. Eyyuboğlu, and Y. Baykal, "Propagation factors of Hermite–Gaussian beams in turbulent atmosphere," *Opt. Laser Technol.*, vol. 42, no. 8, pp. 1344–1348, Nov. 2010, doi: 10.1016/j.optlastec.2010.04.018.

[13] Y. Baykal, M. C. Gökçe, Y. Ata, and H. Gerçekcioğlu, "Correlation of multimode fields in atmospheric turbulence," *J. Opt. Soc. Amer. A, Opt. Image Sci.*, vol. 40, no. 3, p. 462, Feb. 2023, doi: 10.1364/josaa.482588.

[14] Y. Baykal, "Scintillation index for a multimode laser incidence in weak atmospheric turbulence," *Opt. Commun.*, vol. 62, no. 5, pp. 295–299, Jun. 1987, doi: 10.1016/0030-4018(87)90293-8.

[15] S. J. Wang, Y. Baykal, and M. A. Plonus, "Receiver aperture averaging effects for the intensity fluctuation of a beam wave in the turbulent atmosphere," *J. Opt. Soc. Am. A*, vol. 73, no. 6, pp. 831–837, 1983.

[16] M. C. Gökçe, Y. Baykal, Y. Ata, and H. Gerçekcioğlu, "Multimode beam propagation in atmospheric turbulence," in *Proc. NATO Workshop Light Propag. Random Media Impact Wireless Opt. Commun. Syst. Evolving Conditions, NATO STO Centre Maritime Res. Experimentation (CMRE)*, La Spezia, Italy, Aug. pp. 29–31.

[17] C. H. Acevedo, Y. Torres-Moreno, and A. Dogariu, "Spatial intensity correlations of a vortex beam and a perfect optical vortex beam," *J. Opt. Soc. Amer. A, Opt. Image Sci.*, vol. 36, no. 4, p. 518, Mar. 2019, doi: 10.1364/josaa.36.000518.

[18] M. C. Gökçe, Y. Baykal, H. Gerçekcioğlu, and Y. Ata, "Intensity and degree of coherence of vortex beams in atmospheric turbulence," *IEEE J. Quantum Electron.*, vol. 60, no. 6, pp. 1–8, Dec. 2024.

[19] Y. Baykal and H. Gerçekcioğlu, "Field correlations of partially coherent optical beams in underwater turbulence," *J. Opt. Soc. Am. A*, vol. 39, pp. 1187–1192, Jul. 2022, doi: 10.1364/JOSAA.454017.

[20] Y. Baykal, M. C. Gökçe, Y. Ata, and H. Gerçekcioğlu, "Field correlations of multimode optical beams in underwater turbulence," *J. Opt. Soc. Amer. A, Opt. Image Sci.*, vol. 41, no. 6, p. 1037, 2024, doi: 10.1364/josaa.522599.

[21] M. C. Gökçe, Y. Baykal, Y. Ata, and H. Gerçekcioğlu, "Multimode beam propagation through atmospheric turbulence," *J. Quant. Spectrosc. Radiat. Transf.*, vol. 314, Feb. 2024, Art. no. 108857, doi: 10.1016/j.jqsrt.2023.108857.

[22] Y. Baykal and H. Gerçekcioğlu, "Multimode laser beam scintillations in strong atmospheric turbulence," *Appl. Phys. B*, vol. 125, no. 8, p. 152, Jul. 2019, doi: 10.1007/s00340-019-7269-x.

[23] Y. Baykal, "Multimode laser beam scintillations in non-kolmogorov turbulence," *IEEE J. Sel. Areas Commun.*, vol. 33, no. 9, pp. 1883–1889, Sep. 2015, doi: 10.1109/JSAC.2015.2432531.

[24] Ö. F. Sayan, H. Gerçekcioğlu, and Y. Baykal, "Multimode laser beam scintillations in weak atmospheric turbulence for vertical link laser communications," *Waves Random Complex Media*, vol. 32, no. 4, pp. 1890–1902, Jul. 2022, doi: 10.1080/17455030.2020.1841331.

[25] Ö. F. Sayan, H. Gerçekcioğlu, and Y. Baykal, "Hermite Gaussian beam scintillations in weak atmospheric turbulence for aerial vehicle laser communications," *Opt. Commun.*, vol. 458, Mar. 2020, Art. no. 124735, doi: 10.1016/j.optcom.2019.124735.

[26] H. Gercekcioglu, "BER of annular beams in weak oceanic turbulence," *Selcuk Univ. J. Eng., Science Technol.*, vol. 5, no. 3, pp. 262–273, Sep. 2017, doi: 10.15317/scitech.2017.87.

[27] H. Gerçekcioğlu, "Bit error rate of focused Gaussian beams in weak oceanic turbulence," *J. Opt. Soc. Amer. A, Opt. Image Sci.*, vol. 31, no. 9, p. 1963, Aug. 2014, doi: 10.1364/josaa.31.001963.

[28] H. Gerçekcioğlu and Y. Baykal, "Bit error rate of M-pulse position modulated laser beams for vertical links operating in weak oceanic turbulence," *J. Opt.*, vol. 26, no. 10, Oct. 2024, Art. no. 105602, doi: 10.1088/2040-8986/ad44ae.

[29] H. Gerçekcioğlu and Y. Baykal, "Depth dependence of power spectrum in underwater turbulence," *Phys. Scripta*, vol. 97, no. 12, Dec. 2022, Art. no. 125508, doi: 10.1088/1402-4896/aca186.

[30] H. Gerçekcioğlu and Y. Baykal, "Depth dependence of oceanic turbulence optical power spectrum under any temperature and salinity concentration," *Phys. Scripta*, vol. 99, no. 4, Apr. 2024, Art. no. 045511, doi: 10.1088/1402-4896/ad2f05.

[31] Y. Li, Y. Zhang, Y. Zhu, and M. Chen, "Effects of anisotropic turbulence on average polarizability of Gaussian schell-model quantized beams through ocean link," *Appl. Opt.*, vol. 55, no. 19, p. 5234, 2016, doi: 10.1364/ao.55.005234.

[32] Q. Liang, B. Hu, Y. Zhang, Y. Zhu, S. Deng, and L. Yu, "Coupling efficiency of a partially coherent collimating laser from turbulent biological tissue to fiber," *Results Phys.*, vol. 13, Jun. 2019, Art. no. 102162, doi: 10.1016/j.rinp.2019.102162.

[33] V. V. Nikishov and V. I. Nikishov, "Spectrum of turbulent fluctuations of the sea-water refraction index," *Int. J. Fluid Mech. Res.*, vol. 27, no. 1, pp. 82–98, 2000, doi: 10.1615/interjfluidmechres.v27.i1.70.

[34] W. Lu, L. Liu, and J. Sun, "Influence of temperature and salinity fluctuations on propagation behaviour of partially coherent beams in oceanic turbulence," *J. Opt. A, Pure Appl. Opt.*, vol. 8, no. 12, pp. 1052–1058, Dec. 2006, doi: 10.1088/1464-4258/8/12/004.

[35] Y. Li, Y. Zhang, and Y. Zhu, "Oceanic spectrum of unstable stratification turbulence with outer scale and scintillation index of Gaussian-beam wave," *Opt. Exp.*, vol. 27, no. 5, p. 7656, 2019, doi: 10.1364/oe.27.007656.

[36] R. C. Smith and K. S. Baker, "Optical properties of the clearest natural waters (200–800 nm)," *Appl. Opt.*, vol. 20, no. 2, p. 177, 1981, doi: 10.1364/ao.20.000177.

Hamza Gerçekcioğlu received the B.Sc. degree from Hacettepe University, Ankara, Türkiye, in 1996, and the M.Sc. and Ph.D. degrees from Gazi University, Ankara, in 2000 and 2008, respectively. He was a Lecturer and a Researcher with the Department of Electronic Engineering, Kırıkkale University, in areas of communication systems, fiber optics, and telecommunication networks. His Ph.D. thesis is in the field of atmospheric turbulence and free space optics communication systems. Currently, he is with the Ministry of Transport and Infrastructure, Ankara. He has published a lot of SCI journals and proceedings articles. He was the President of the Prime Ministry Undersecretaries for Maritime Affairs, Communications and Electronics Department, and managed Vessel Traffic Control and Infrastructure of Communications Systems of Turkish Territorial Waters and as the Deputy Director General of the Ministry of Transport Maritime Affairs and Communications, Directorate General of Aeronautics and Space Technologies. With optical wave propagation in atmospheric and oceanic medium, his research interests include aerial vehicle and satellite laser and RF communications.

Yahya Baykal received the Ph.D. degree from the Electrical Engineering and Computer Sciences Department, Northwestern University, Evanston, IL, USA. He is currently a Professor with the Department of Electrical-Electronics Engineering, Çankaya University, Ankara, Türkiye. He is the author of more than 225 SCI journal articles and more than total 300 publications. His research interests include optical communication, optical wave propagation in atmospheric, underwater media, and telecommunications infrastructure.

Muhsin Caner Gökçe received the M.S. degree in electronics engineering from Ankara University, Ankara, Türkiye, in 2012, and the Ph.D. degree in electronic and communication engineering from Çankaya University, Ankara, in 2016. He is currently an Associate Professor with the Department of Electrical-Electronics Engineering, TED University, Ankara. He is currently employed as a Post-Doctoral Researcher with the Department of Geoscience and Remote Sensing, Delft University of Technology, The Netherlands. His research interests include optical wireless communication and optical beam propagation through turbulent media.